

****Volume Title****

*ASP Conference Series, Vol. **Volume Number***

****Author****

© ****Copyright Year**** *Astronomical Society of the Pacific*

Reviewing the observational evidence against long-lived spiral arms in galaxies

Eric E. Martínez-García¹ & Ivanio Puerari¹

¹*Instituto Nacional de Astrofísica, Óptica y Electrónica (INAOE), Aptdo. Postal 51 y 216, 72000 Puebla, Pue., México*

Abstract.

We review Foyle et al. (2011) previous results, by applying a Fourier intensity phases method to a nine object sample of galaxies. It was found that two of the objects (NGC 628 and NGC 5194), with strong two-arm patterns, present positive evidence for long-lived spirals. Only one of the objects (NGC 3627) shows the contrary evidence. As determined by an analysis of resolved mass maps, the rest of the objects can not be included in the analysis because they belong to flocculent and multi-arm type of spiral arms, which are not described by density wave theory.

1. Introduction

As implied by the density wave (DW) theory, spiral patterns should be thought of as dynamical features that are stationary in a corotating frame. If such spiral arms trigger star formation (SF), some observational tracers for different stages of the SF sequence should show a spatial ordering (Foyle et al. 2011).¹ From upstream to downstream in the corotating frame: dense HI emission, CO emission tracing molecular hydrogen gas, $24\mu\text{m}$ emission tracing enshrouded SF, and UV emission tracing unobscured young stars. Foyle et al. (2011) analyzed a sample of 12 nearby spiral galaxies, with grand-design, flocculent, and barred objects. A cross-correlation method was adopted. Their findings argue for little evidence supporting the DW scenario, even for the grand-design objects.

Our research involves the analysis of spiral galaxies in search for this sequence of SF, by adopting the Fourier method of Puerari & Dottori (1997). As in Foyle et al. (2011), the observational data consists on high-quality maps of neutral gas (HI) from THINGS (Walter et al. 2008); molecular gas (CO) from HERACLES (Leroy et al. 2009); $24\mu\text{m}$ emission from Spitzer (SINGS, Kennicutt et al. 2003); FUV images from GALEX (Gil de Paz et al. 2007); and $3.6\mu\text{m}$ emission from Spitzer (SINGS, Kennicutt et al. 2003). Nine nearby spiral galaxies have common data in all the aforementioned surveys and were selected (NGC 628, 2403, 2841, 3351, 3521, 3627, 5055, 5194 and NGC 6946). With the exception of NGC 6946, all the objects also have also cross-sections in SDSS (York et al. 2000).

¹ Besides the discussed SF sequence, azimuthal age/color gradients are also expected across spiral arms. These gradients are indeed present in some objects as has been probed by Gonzalez & Graham (1996), Martínez-García et al. (2009a,b), and Martínez-García & González-Lópezlira (2011, 2013)

2. Candidates that may host density waves

Not all types of spirals can be explained by DW theory. Only the symmetric grand-design objects may harbor mass structure with nearly constant patterns speeds, i.e., density waves. Thereby multi-armed and flocculent spirals are naturally excluded as stellar DW candidates (Efremov 2011; Martínez-García & González-Lópezlira 2013). In order to discern whether these structures are present in the disks of our sample of galaxies, we adopt the following method. Resolved maps of stellar mass were obtained by extending the Zibetti, Charlot & Rix (2009) method to the $3.6\mu\text{m}$ -band of IRAC-Spitzer. This was done because these near-infrared (NIR) images are available for our entire sample of objects, in addition to its quality. The dust emission model of da Cunha et al. (2008) was adopted to include dust radiation into account. A Monte Carlo library of stellar population synthesis (SPS) models, and dust radiation models was obtained as in Zibetti, Charlot & Rix (2009). An energy balance condition (da Cunha et al. 2008) was applied so that all the radiation absorbed in the ISM, and stellar birth clouds, is re-radiated in the infrared for wavelengths longer than $2.5\mu\text{m}$. A look-up table was then derived for the $(g - i)$ color, the $(i - 3.6\mu\text{m})$ color, and the mean $M/L_{(3.6\mu\text{m})}$ ratio. This look-up table was compared with SDSS² and $3.6\mu\text{m}$ photometry in a pixel-by-pixel basis, thereby obtaining a map of the $M/L_{(3.6\mu\text{m})}$ ratio. These maps were transformed to absolute mass maps with distances obtained from the literature.

The two-dimensional mass maps were then analyzed to select those with a strong two-armed spiral pattern ($m = 2$). This was done with 2D FFT methods, the same used for pitch angle measurements (e.g., Considere & Athanassoula 1982; Puerari & Dottori 1992; Saraiva Schroeder et al. 1994; Davis et al. 2012). The results are shown in figure 1, where we can see that only three objects (NGC 628, NGC 3627 and NGC 5194) show signs of strong $m = 2$ spiral patterns. These objects were considered for the analysis of azimuthal phases of intensity as described below.

3. Fourier method of azimuthal phases

Puerari & Dottori (1997) method is based on computing the Fourier transform of the form

$$\hat{f}(m) = \int_{-\pi}^{\pi} I_R(\theta) e^{-im\theta} d\theta, \quad (1)$$

where I_R is the intensity of radiation, and the phase

$$\Phi = \tan^{-1} \left\{ \frac{\text{Re}[\hat{f}(m)]}{\text{Im}[\hat{f}(m)]} \right\}, \quad (2)$$

for two-armed spiral modes, i.e., $m = 2$. This implies that twice the period of the analyzed signal is contained within a 2π radians interval, i.e., a π radians symmetry. The azimuthal phases were computed for the HI, CO, $24\mu\text{m}$, and FUV data. All data were degraded to the CO (Heracles, Leroy et al. 2009) resolution. For shock-induced star formation in a DW scenario (Roberts 1969), before the corotation, we expect to

²The Johnson's V and I filters were used for NGC 6946.

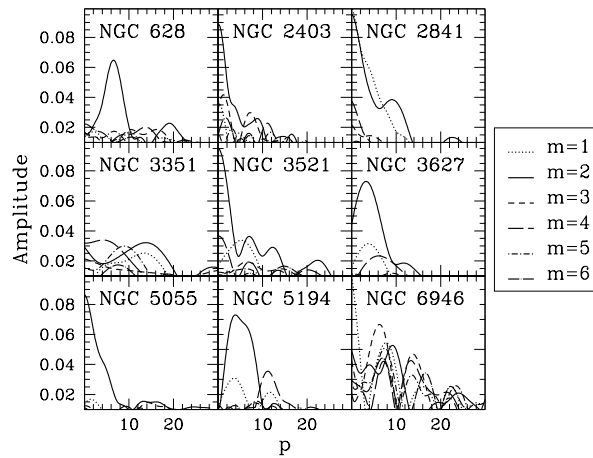


Figure 1. Amplitudes vs. p frequencies (absolute values), obtained with 2D FFT methods, for the resolved mass maps in our sample of objects. The p frequency is the one associated with the pitch angle of the object (see, e.g., Saraiva Schroeder et al. 1994).

find a higher phase value for the HI data, and lower phase values for the CO, $24\mu\text{m}$, and FUV data, in an ordered sequence. The phases most coincide near corotation, and invert their order afterwards.

4. Results

For the three objects analyzed, it was found that none of the HI, and FUV phase plots, show the expected sequence if DW's are indeed present in the disk. Although, if the HI emission is contaminated by the gas photodissociated by recently formed stars, it would not trace the compressed gas (Louie et al. 2013). For NGC 628 and NGC 5194, it was found that the CO and $24\mu\text{m}$ emission show the expected sequence for the DW scenario. For NGC 628, the CO- $24\mu\text{m}$ phase shift coincides with the expectations up to the place where the spiral arms seem to end, as inferred from the mass map. For NGC 5194, the phase shifts agree with a DW scenario for most of its spiral extension (see figure 2). No consistent phases were found for NGC 3627.

5. Conclusions

We analyzed a sample of nine objects, with available data in HI, CO, $24\mu\text{m}$, and FUV. Based on SDSS, and $3.6\mu\text{m}$ photometry, resolved mass maps were obtained. In these mass maps, three objects (NGC 628, NGC 3627, and NGC 5195) show a strong spiral pattern with $m = 2$. After applying a Fourier method to calculate azimuthal phases (Puerari & Dottori 1997), two of the objects, NGC 628, and NGC 5194, showed indications of a corotation (at least for the phase shift between CO and $24\mu\text{m}$). This is clear sign of a dominant pattern speed with a constant value, i.e., long-lived spirals.

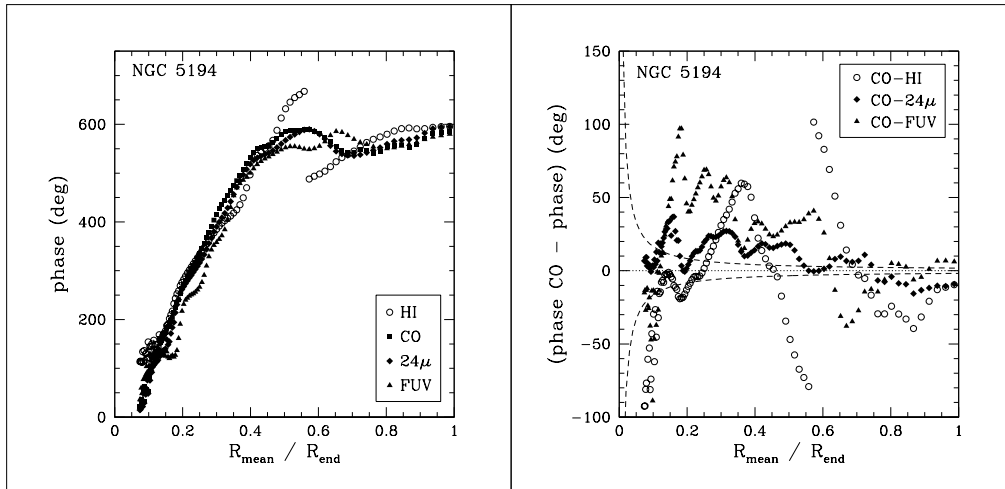


Figure 2. Azimuthal intensity phases for NGC 5194. Left: Azimuthal phases (y-axis), vs., normalized radius $R_{\text{mean}}/R_{\text{end}}$ (x-axis), where R_{end} indicates the end of the spirals in the $3.6\mu\text{m}$ image. Right: Differences between the phases in CO and other tracers (y-axis), vs., normalized radius $R_{\text{mean}}/R_{\text{end}}$ (x-axis). The long-dashed line indicates the resolution of the data.

Acknowledgments. EMG acknowledges support from the mexican institution CONACYT.

References

- Considerere, S., & Athanassoula, E. 1982, *A&A*, 111, 28
da Cunha, E., Charlot, S., & Elbaz, D. 2008, *MNRAS*, 388, 1595
Davis, B. L., Berrier, J. C., Shields, D. W., et al. 2012, *ApJS*, 199, 33
Efremov, Y. N. 2011, *Astronomy Reports*, 55, 108
Foyle, K., Rix, H.-W., Dobbs, C. L., Leroy, A. K., & Walter, F. 2011, *ApJ*, 735, 101
Gonzalez, R. A., & Graham, J. R. 1996, *ApJ*, 460, 651
Gil de Paz, A., Boissier, S., Madore, B. F., et al. 2007, *ApJS*, 173, 185
Kennicutt, R. C., Jr., Armus, L., Bendo, G., et al. 2003, *PASP*, 115, 928
Leroy, A. K., Walter, F., Bigiel, F., et al. 2009, *AJ*, 137, 4670
Louie, M., Koda, J., & Egusa, F. 2013, *ApJ*, 763, 94
Martínez-García, E. E., González-Lópezlira, R. A., & Bruzual-A, G. 2009a, *ApJ*, 694, 512
Martínez-García, E. E., González-Lópezlira, R. A., & Gómez, G. C. 2009b, *ApJ*, 707, 1650
Martínez-García, E. E., & González-Lópezlira, R. A. 2011, *ApJ*, 734, 122
Martínez-García, E. E., & González-Lópezlira, R. A. 2013, *ApJ*, 765, 105
Puerari, I., & Dottori, H. A. 1992, *A&AS*, 93, 469
Puerari, I., & Dottori, H. 1997, *ApJ*, 476, L73
Roberts, W. W. 1969, *ApJ*, 158, 123
Saraiva Schroeder, M. F., Pastoriza, M. G., Kepler, S. O., & Puerari, I. 1994, *A&AS*, 108, 41
Walter, F., Brinks, E., de Blok, W. J. G., et al. 2008, *AJ*, 136, 2563
York, D. G., Adelman, J., Anderson, J. E., Jr., et al. 2000, *AJ*, 120, 1579
Zibetti, S., Charlot, S., & Rix, H.-W. 2009, *MNRAS*, 400, 1181